Thermally Stable Antireflective Coatings Based on Nanoporous Organosilicate Thin Films

Suhan Kim,[†] Jinhan Cho,[‡] and Kookheon Char*,[†]

School of Chemical & Biological Engineering, NANO Systems Institute - National Core Research Center (NCRC), Seoul National University, Seoul 151-744, Korea, and School of Advanced Materials, Kookmin University, Seoul 136-702, Korea

Thermally stable nanoporous organosilicate thin films were realized by the microphase separation of pore-generating polymers mixed with an organosilicate matrix to be antireflective coatings (ARCs), for which a thin film with a refractive index (*n*) of 1.23 for zero reflection is required. The refractive index of such nanoporous organosilicate films can be tuned from 1.39 down to 1.23 by incorporating nanopores within the films. With a nanoporous single layer with $n \sim 1.23$, the light transmittance of the glass above 99.8% was achieved in the visible range ($\lambda \sim 550$ nm). To overcome the limitation on the narrow wavelength for high transmittance imposed by a single antireflective nanoporous thin film, bilayer thin films with different refractive indices were prepared by placing a high refractive index layer with a refractive index of 1.45 below the nanoporous thin film. UV−vis transmittance of a glass coated with the bilayer films was compared with nanoporous single-layer films and it is demonstrated that the novel broadband antireflection coatings in a wide range of visible wavelength can be easily obtained by the organosilicate bilayer thin films described in this study. Also, ARCs developed in this study demonstrate excellent AR durability owing to the hydrophobic nature of the organosilicate matrix.

Introduction

Antireflective coatings (ARCs) have recently gained great interest for their possible applications in optical and display devices since the antireflection coating not only removes ghost images but also enhances the transmittance of light. Based on the thin film optics, the ARC is designed as a quarter-wave optical thickness for a wavelength (λ) of interest with a refractive index (*n*) given by $n = (n_0 \cdot n_{sub})^{1/2}$, where n_0 is the refractive index of air and n_{sub} is the refractive index of a substrate. For applications to display devices such as CRTs, PDPs, and LCDs, the ARC should be designed to achieve the highest transmittance in the visible region. The wavelength at zero reflectance can be easily tuned by controlling the coating thickness and the zero reflectance can be achieved by adopting a coating material with a refractive index close to 1.23 for a glass substrate with a refractive index of 1.52. However, the lowest refractive index among homogeneous one-phase materials is above 1.35 for magnesium fluoride. In recent years, zero reflection ARCs for glasses were achieved by preparing nanoporous films, which enables continuous reduction of the refractive index by incorporating nanopores (with $n = 1$) within the films. The nanoscale pores within the ARC film are small enough to be transparent for visible light.

Earlier nanoporous ARC films were achieved by the polymer blend approach. Nanoporous films were obtained by removing one phase of the polymer blend after the spin casting of a polymer blend solution.[1] Another approach to realize nanoporous polymeric ARCs is to use the layer-by-layer assembly method. After deposition of polymers by the layer-by-layer deposition method, the post acid treatment induced nanoporous structure within the

film by altering the polymer conformation.[2] These previous approaches lower the effective refractive index and show good antireflective properties. However, the polymer-based antireflective approach can have poor durability owing to soft polymeric materials and weak adhesion to the substrate. Hattori suggested the silica particle coating at the surface for the ARC by depositing silica particles with a diameter equivalent to the quarter-wave optical thickness.[3] Gombert et al. also suggested antireflective coatings with periodic or stochastic subwavelength surface-relief structure based on the sol−gel process. It is noted that these approaches based on inorganic materials cannot achieve high transmittance over 99.5%.[4]

In the present study, we utilize nanoporous organosilicate materials[5−10] as another option for ARCs since nanoporous organosilicate films could achieve low refractive index as well as excellent antireflective durability. We can easily lower the refractive index of nanoporous organosilicate films to 1.23, which is the required refractive index for the zero reflection on a glass substrate, simply by varying the pore-generating material (porogen) loading. UV−vis transmittance of glass coated with prepared nanoporous organosilicate films was also investigated for application to antireflection coatings. With a nanoporous

---

* To whom correspondence should be addressed. E-mail: khchar@plaza.snu.ac.kr.

† School of Chemical and Biological Engineering, Seoul National University.

‡ School of Advanced Materials, Kookmin University.

(1) Walheim, S.; Schaffer, E.; Mlynek, J.; Steiner, U. *Science* **1999**, *283*, (5401), 520−522.

(2) Hiller, J.; Mendelsohn, J. D.; Rubner, M. F. *Nat. Mater.* **2002**, *1* (1), 59−63.

(3) Hattori, H. *Adv. Mater.* **2001**, *13* (1), 51−54.

(4) Gombert, A.; Glaubitt, W.; Rose, K.; Dreibholz, J.; Bläsi, B.; Heinzel, A.; Sporn, D.; Döll W.; Wittwer, V. *Thin Solid Films* **1999**, *351*, 73−78.

(5) Toivola, Y.; Kim, S.; Cook, R. F.; Char, K.; Lee, J. K.; Yoon, D. Y.; Rhee, H. W.; Kim, S. Y.; Jin, M. Y. *J. Electrochem. Soc.* **2004**, *151* (3), F45−F53.

(6) Huang, Q. R.; Volksen, W.; Huang, E.; Toney, M.; Frank, C. W.; Miller, R. D. *Chem. Mater.* **2002**, *14* (9), 3676−3685.

(7) Nguyen, C. V.; Carter, K. R.; Hawker, C. J.; Hedrick, J. L.; Jaffe, R. L.; Miller, R. D.; Remenar, J. F.; Rhee, H. W.; Rice, P. M.; Toney, M. F.; Trollsas, M.; Yoon, D. Y. *Chem. Mater.* **1999**, *11* (11), 3080−3085.

(8) Yim, J. H.; Lyu, Y. Y.; Jeong, H. D.; Song, S. A.; Hwang, I. S.; Hyeon-Lee, J.; Mah, S. K.; Chang, S.; Park, J. G.; Hu, Y. F.; Sun, J. N.; Gidley, D. V. *Adv. Funct. Mater.* **2003**, *13* (5), 382−386.

(9) Yim, J. H.; Baklanov, M. R.; Gidley, D. W.; Peng, H. G.; Jeong, H. D.; Pu, L. S. *J. Phys. Chem. B* **2004**, *108* (26), 8953−8959.

(10) Yim, J. H.; Seon, J. B.; Jeong, T. D.; Pu, L. Y. S.; Baklanov, M. R.; Gidley, D. W. *Adv. Funct. Mater.* **2004**, *14* (3), 277−282.

---

single layer of $n \sim 1.23$, the maximum transmittance above 99.8% in the visible range was achieved. However, the disadvantage of the single-layer coating is that the single-layer coating yields high transmittance only in the narrow wavelength region. Accordingly, a more rewarding approach is to use multiple layers by varying reflectance of each layer. To achieve broadband ARCs, we prepared bilayer ARC films by inserting a high refractive index layer based on an organosilicate MTMS:TEOS (1:9) copolymer with a refractive index of 1.45 just under the nanoporous top layer. As a result, we propose novel broadband bilayer antireflective coatings with improved transmittance over the wide wavelength region.

Experimental Section

Materials. A poly(methyl silsesquioxane) (PMSSQ) copolymer used as a matrix material to realize nanoporous thin films was synthesized by the sol–gel reaction with methyltrimethoxysilane (MTMS, Aldrich) and 1,2-bis(trimethoxysilyl)ethane (BTMSE, Aldrich).[11] The feed ratio of MTMS and BTMSE was 90/10 by mol %. A tetra-functional block copolymer (Tetronic 150R1, BASF) was used as a porogen. Photoacid generator (triphenylsulfonium trifluoromethanesulfonate, Hayashi Pure Chemical) (PAG) was used to lower the refractive index of PMSSQ copolymer. For the preparation of bilayer AR films with gradient refractive indices, MTMS and tetraethoxyorthosilicate (TEOS, Aldrich) were copolymerized with molar ratios of 1:9, 2:8, and 3:7.

Film Preparation. The PMSSQ copolymer containing 1 wt % of PAG was mixed with 0, 20, and 40 wt % of porogens in methyl isobutyl ketone (MIBK). The concentration of prepared matrix/porogen mixtures was varied from 4.5 to 9.0 wt % to change the film thickness. The solutions were spin-coated on glasses at 3000 rpm for 30 s. To realize nanopores within the films, spin-coated films were calcined at 420 °C for 1 h after UV irradiation for 10 min at the dosage of 2.8 mW/cm². To prepare bilayer films, an organosilicate copolymer with a high refractive index was first dissolved in *n*-butanol and spin-coated on a glass and cured at 200 °C. The matrix/porogen mixture solution was then spin-coated on top of a cured high refractive index layer and calcined at 420 °C for 1 h.

Characterization. The thicknesses and refractive indices of nanoporous organosilicate films on silicon wafers were measured by an ellipsometer (Gaertner Scientific Corp., L2W15S830) equipped with a He–Ne laser (wavelength of 632.8 nm). The measured refractive index is thus valid for 632.8 nm but the measured value would remain valid in the visible region. UV–vis transmittance was collected at normal incidence with a Perkin-Elmer Lambda 35 UV–vis spectrometer. The cross-sectional images of ARC films were examined by transmission electron microscopy (JEOL, JEM-3000F) (TEM) and field emission scanning electron microscopy (Philips, XL30FEG) (FE-SEM). Small-angle neutron scattering (SANS) measurements were conducted at the NG3 beamline of the National Institute of Standards and Technology Center for Neutron Research. The sample-to-detector distance was 133 cm. The neutron wavelength was 6 Å with a $\Delta\lambda/\lambda$ spread of 0.15. A stack of eight thin films were placed inside a custom-built flow scattering cell sealed between two quartz windows. Saturated d8-toluene vapor was delivered through the vacuum-tight sample cell with 10 sccm at 25 °C. We collected the SANS data for 10 min after treating the film stack within d8-toluene. X-ray reflectivity (XRR) experiments were carried out at the 3C2 beamline in Pohang Light Source. The X-ray wavelength was 1.54 Å and the fwhm of the X-ray beam was 0.003° by placing a pair of Si-channel cuts in front of the 1-D detector to enhance the spatial resolution. The reflectivity of each sample was measured both in air and under a saturated toluene environment for porosity analysis. Collected data were fitted using the Parret32 program.
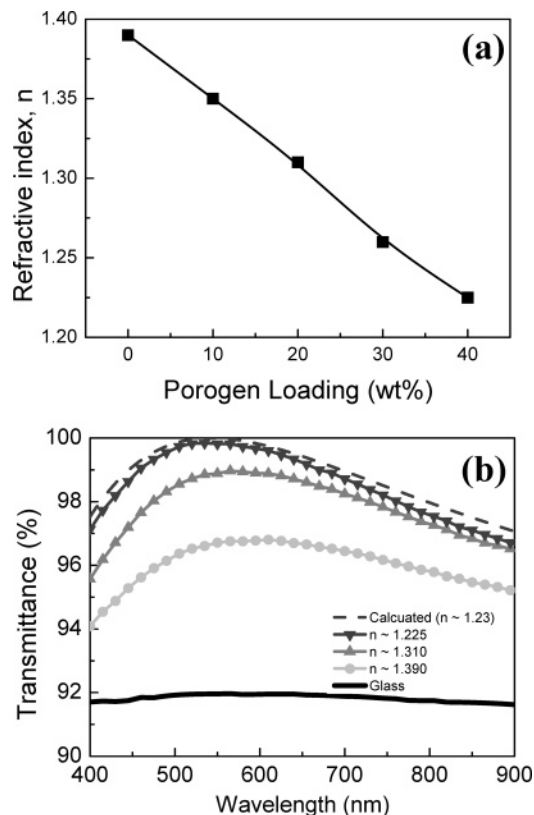
(11) Kim, S.; Toivola, Y.; Cook, R. F.; Char, K.; Chu, S. H.; Lee, J. K.; Yoon, D. Y.; Rhee, H. W. *J. Electrochem. Soc.* **2004**, *151* (3), F37–F44.

Figure 1. (a) Change in refractive indices of porous films as a function of porogen loading. When 40 wt % of porogen is introduced, the refractive index for nanoporous organosilicate film decreases down to 1.23, which satisfies the requirement for the zero reflectance on a glass. (b) UV–vis transmittance for glasses coated with organosilicate films with different refractive indices at both sides. As the refractive index is decreased, the maximum transmittance increases. When the refractive index of a nanoporous film was 1.23, the ARC glass shows the maximum transmittance above 99.8%.

Results and Discussion

Refractive indices of prepared films were measured with an ellipsometer and plotted against porogen loading, as shown in Figure 1a. As the porogen loading is increased, the refractive index of the PMSSQ copolymer decreases from 1.39 to 1.23, respectively. At a 40 wt % of porogen loading, we could obtain a nanoporous organosilicate film with a refractive index of 1.23, which is required for the zero reflection against a glass substrate. Among prepared porous films, porous films with 0, 20, and 40 wt % porogen loadings were selected to evaluate the refractive index of a film for the antireflective effect. We found that the refractive indices for the chosen porous films were 1.39, 1.31, and 1.23, respectively. To achieve antireflective properties in the visible region, the coating thickness of porous films was adjusted to about 110 nm. UV–vis transmittance of the glasses coated with the porous films was measured in the wavelength range from 400 to 900, as shown in Figure 1b. Glasses coated with porous organosilicate films show considerably high transmittance compared with the noncoated pristine glass. The nonporous film with a refractive index of 1.39 also yields the high transmittance of 96.68%. As the porogen loading is increased, the maximum transmittance of glasses coated with the porous films with 20 and 40 wt % porogen loadings became 98.99% and 99.85%, respectively. The dashed line in Figure 1b is the calculated transmittance curve based on the characteristic matrix theory[12] for ARC films with a refractive index of 1.23 and a film thickness of 110 nm. The calculated transmittance is in good agreement with the measured values.

The wavelength at the maximum transmittance (λ_{max}) can be generally controlled by varying the film thickness since λ_{max} is linearly dependent on the film thickness, $\lambda_{max} = 4nd$, where n is the refractive index of a film and d is the film thickness. The thickness of porous organosilicate films is easily controlled by varying solution concentration. As the solution concentration is increased from 4.5 to 9.0 wt %, the film thickness increases from 86 to 188 nm. In our spin-on organosilicate system, the film thickness is almost linearly dependent on the solution concentration, as shown in Figure 2a. To confirm the effect of film thickness, the transmittance for porous films with film thicknesses varying from 86 to 188 nm was measured and plotted in Figure 2b. The wavelength at the maximum transmittance moves to higher wavelength as the film thickness is increased. When we plot the wavelength at maximum transmittance (λ_{max}) as a function of film thickness in Figure 2c, the experimental data are in good agreement with the solid line based on $\lambda_{max} = 4nd$. Consequently, simple and precise control of both porogen amount and film thickness allows us to design optical ARC films.

At the 40 wt % porogen loading within the film, we can achieve the maximum transmittance of 99.85%. With this nanoporous film, we characterize the porous structure with XRR as well as with SANS. Values for the absolute porosity for porous films can be obtained from XRR experiments with and without toluene vapor treatment. Figure 3 shows the XRR curves measured both in air and under saturated toluene as a function of q ($q = (4\pi/\lambda)\sin\theta$, Å^{-1}). From the XRR curve measured in air, we can obtain the average electron density, the density of a film, the surface roughness, and the film thickness, as listed in Table 1. The average electron density is obtained from the critical angle of a porous film where the intensity of reflectivity starts to drop sharply. The density of a porous film is calculated from the combination of the average electron density and the atomic composition of the film (Si:O:C:H =15.8:23.8:15.8:44.6). By fitting the Kessing fringe pattern and the reflectivity slope, we obtain information on surface roughness as well as film thickness. The nanoporous film with a 40 wt % of porogen loading yields a smooth surface with a surface roughness of 0.6 nm and the calculated film thickness is 104.2 nm, which is comparable to the film thickness of 110 nm measured by ellipsometry. The XRR measurement was also conducted after exposure to toluene vapor, which allows us to obtain the absolute porosity. The nanoporous film was placed in a vacuum-sealed chamber filled with saturated toluene vapor. Toluene vapor easily penetrates organosilicate films and condenses inside the pores due to the capillary condensation.[13–15] By treatment of the film with toluene vapor, the average electron density and the film density increase due to the sorption of toluene within the film. The comparison between two densities obtained from the XRR data measured both in air and after toluene sorption quantitatively yield information on the pore volume by solving two equations below,

$$\rho_{air} = \rho_{wall}(1 - P) \tag{1}$$

$$\rho_{saturated} = \rho_{wall}(1 - P) + \rho_{toluene}P \tag{2}$$

where ρ_{air}, ρ_{wall}, $\rho_{saturated}$, and $\rho_{toluene}$ are the film density measured in air, the density of wall material separating pores, the film density measured in a toluene-saturated environment, and the density of toluene, respectively. Calculated porosity of the porous film with a 40 wt % porogen loading is 46.6%, which is slightly
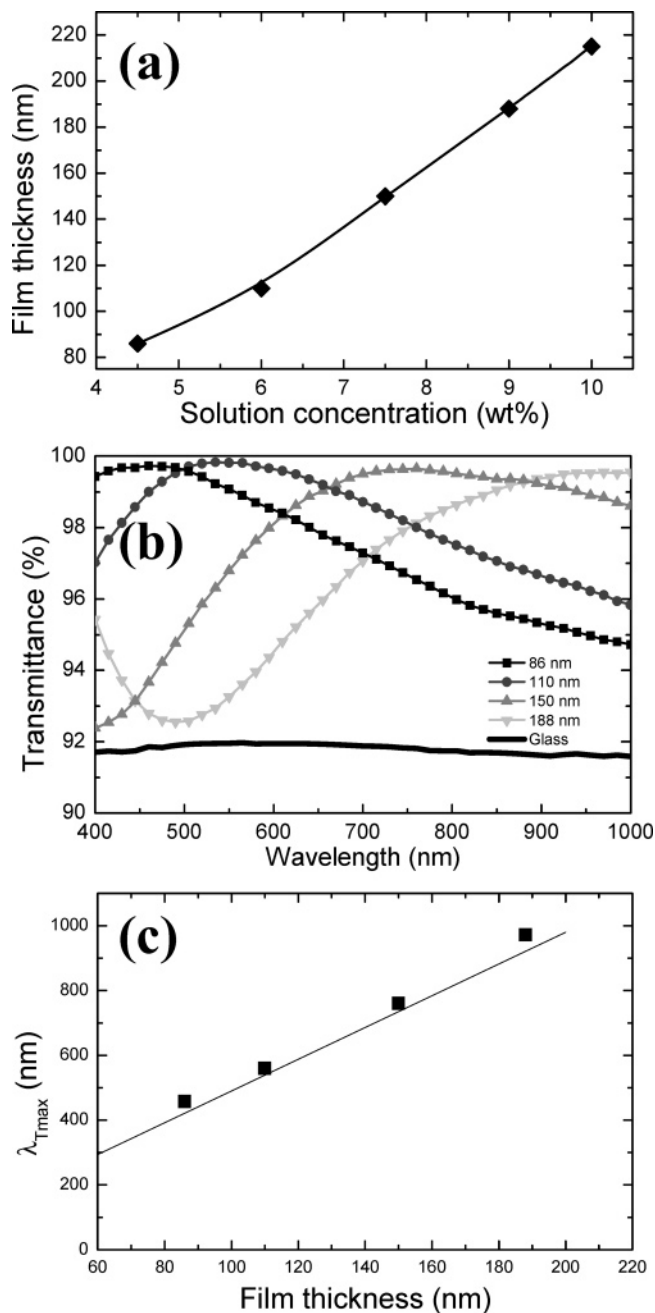
Figure 2. (a) Changes in film thickness as a function of solution concentration containing 40 wt % of porogens. (b) The wavelength at the maximum transmittance of glasses coated with porous films loaded with 40 wt % of porogen shifts to higher wavelength with the increase in ARC film thickness. (c) Dependence of wavelength at the maximum transmittance on film thickness. Calculated wavelength at the maximum transmittance ($\lambda_{Tmax} = 4nd$, where n is the refractive index of a coating material and d is the film thickness) is also plotted against the film thickness, showing good agreement with the measured data.

larger than the relative porosity calculated based on the Lorentz–Lorenz equation using the refractive indices measured by ellipsometry. We believe that this is because the toluene vapor penetrates even the micropores within the matrix material and the porosity measured by the XRR experiment includes the pores

(12) Macleod, H. A. *Thin-Film Optical Filters: Third Edition*; Institute of Physics Publishing: London, 2001.

(13) Lee, H. J.; Soles, C. L.; Liu, D. W.; Bauer, B. J.; Wu, W. L. *J. Polym. Sci., Part B: Polym. Phys.* **2002**, *40* (19), 2170−2177.

(14) Lee, H. J.; Soles, C. L.; Liu, D. W.; Bauer, B. J.; Lin, E. K.; Wu, W. L.; Grill, A. *J. Appl. Phys.* **2004**, *95* (5), 2355−2359.

(15) Soles, C. L.; Lee, H. J.; Hedden, R. C.; Liu, D. W.; Bauer, B. J.; Wu, W. L. *Polym. Microelectron. Nanoelectron.* **2004**, *874*, 209−222.
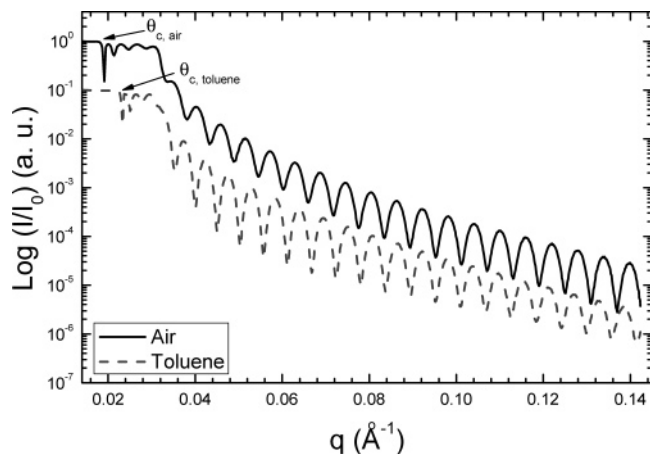
Figure 3. X-ray reflectivity data obtained from a single-layer nanoporous organosilicate thin film measured both in air and under a saturated toluene environment.

Table 1. Physical Properties of a Single-Layer Nanoporous Film with a 40 wt % Porogen Loading from the XRR Experiments Measured Both in Air and under Saturated Toluene Environment

environment	ρ_e (e^{-1}/Å^3)	density (g/cm^3)	thickness (nm)	roughness (nm)	porosity (%)
air	0.235	0.750	104.2	0.6	46.6
toluene	0.362	1.153	105.4	1.1	

created by the calcination of porogens as well as the micropores inherent to the matrix material. This is again confirmed by the XRR experiment on the nonporous PMSSQ copolymer film which contains 5.6% of absolute porosity (data not shown). From the XRR experiments, we confirm that the ARC film contains 46.6% of porosity and the pores effectively created reduce the density of ARC film.

The reduction in the film density allows the low refractive index of 1.23 to meet the requirement of zero reflection for glasses. However, the required refractive index for the zero reflectance is only valid for a homogeneous one-component film. This is to say that the generated pores should be much smaller than the wavelength of interest to eliminate any possible scattering off the pores. We thus analyze pore size and pore size distribution of the porous film by SANS. In Figure 4a, the SANS profile obtained from a 2D SANS pattern measured for the nanoporous organosilicate film with a 40 wt % porogen loading is shown with open square symbols. Solid line is obtained by fitting the data based on the polydisperse hard sphere (PHS) model which calculates the scattered intensity for a population of polydisperse spheres, including the hard sphere interaction between particles. In this model, the Schulz distribution is employed to describe the polydispersity in pore diameter. The Schulz distribution has the form

$$n(r) = \left(\frac{\alpha}{\bar{r}}\right)^{\alpha} \frac{r^{\alpha-1}}{\Gamma(\alpha)} \exp\left(-\frac{\alpha}{\bar{r}}r\right) \tag{3}$$

where $\bar{r}$ is the average pore radius, α is $1/\delta^2$, and δ is the polydispersity. Polydispersity (δ) is the term defined in the Schulz distribution ranging from 0 to 1. When the δ value is close to zero, the pore size distribution becomes monodisperse. The δ value close to unity implies that the pore size distribution is quite broad. Average pore radius is 1.1 nm and the polydispersity δ is found to be 0.76. We also calculated volume distribution of pores based on the Schulz distribution and plotted the volume distribution of pores against pore radius, as shown in Figure 4b.
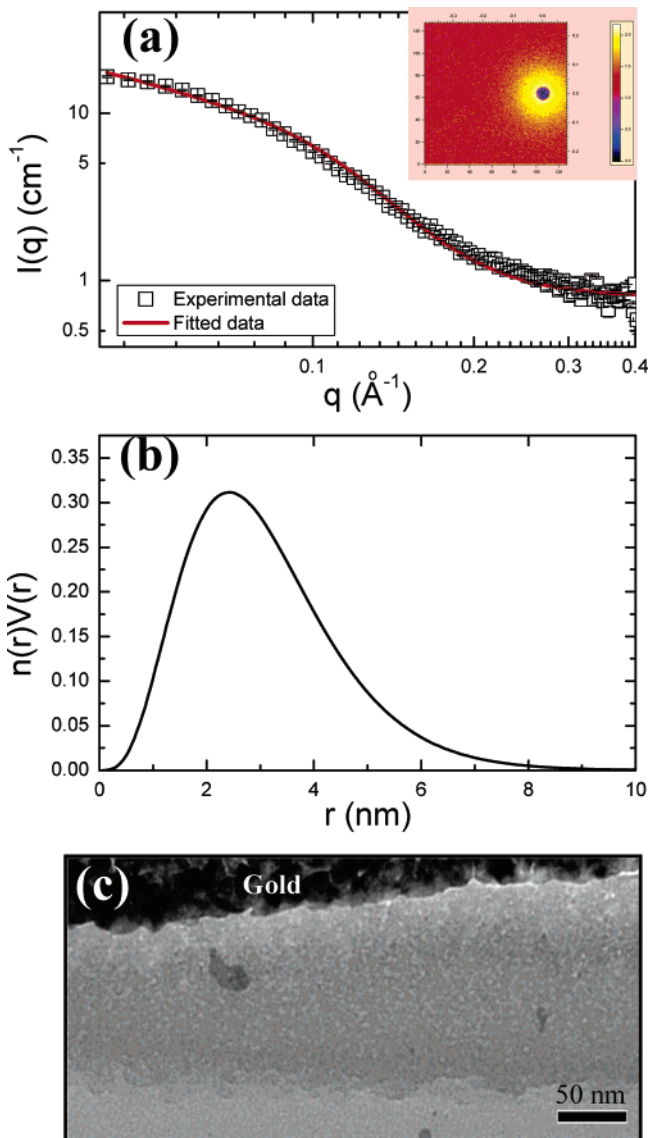

Figure 4. (a) SANS scattering profile obtained from a 2D SANS pattern measured for a porous film with a 40 wt % of porogen loading. Solid line is obtained by fitting the data using the PHS model. (b) Volume-averaged pore size distribution obtained from the SANS analysis. (c) Cross-sectional TEM image for nanoporous films with a 40 wt % of porogen loading.

Average radius from the volume distribution of pores is 3.0 nm. Although the estimated pore radius is somewhat polydisperse, the pore radius was below 10 nm, which is much smaller than the wavelength of light ($\lambda = 400-900$ nm). Consequently, the prepared nanoporous organosilicate film satisfies all the requirements for ARCs without any parasitic scattering due to nanopores generated within the films. We also obtained the cross-sectional TEM image of the nanoporous organosilicate film with a 40 wt % porogen loading to confirm the size of nanopores in a different way. A black layer on top of the image in Figure 4c is the sputtered gold layer, indicating the film/air interface. The TEM image confirms the SANS data representing nanopores with 2−3 nm in radius, evenly distributed across the film thickness.

Although a single nanoporous organosilicate thin film itself yields high transmittance of light, the range of wavelength for the high transmittance is quite limited. For applications in displays, for example, the difference in the transmittance at different wavelengths in the visible region could result in the distortion of color contrast. To overcome this limitation, broadband ARC
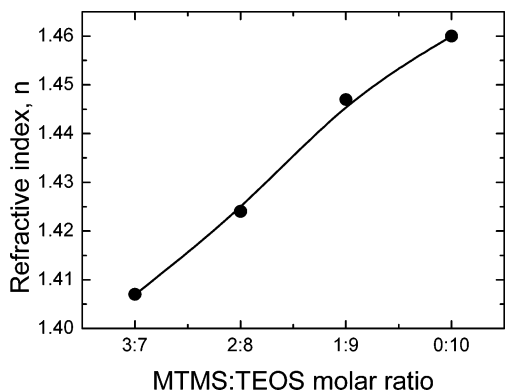
Figure 5. Changes in the refractive index of MTMS:TEOS copolymers as a function of MTMS:TEOS molar ratio.

Figure 6. A cross-sectional SEM image for a bilayer ARC film with a nanoporous organosilicate film with $n \sim 1.23$ on top of a MTMS:TEOS copolymer with $n \sim 1.45$. Note that different textures for the top and the bottom layers are clearly visible, confirming the nanoporous top layer.

is required. Broadband ARC can thus be achieved by realizing the gradient refractive index within the film.[1,2,12] When we employ a bilayer ARC film, the desired refractive index and film thickness for the bottom reflective layer is 1.44 and 90 nm, respectively, when we calculate the transmittance in the visible region based on the characteristic matrix theory.[12] When we employ a bilayer ARC film, the desired refractive index and film thickness for the bottom reflective layer is 1.44 and 90 nm, respectively, when we calculate the transmittance in the visible region based on the characteristic matrix theory.[12] We thus designed MTMS:TEOS copolymers to serve as a bottom layer with a refractive index of 1.44 for the broadband ARCs since the refractive index of silicon dioxide (SiO_2) prepared with TEOS is 1.46 while the refractive index of MSSQ derived from MTMS is 1.387. MTMS: TEOS copolymers with molar ratios of 1:9, 2:8, and 3:7 were synthesized by the sol–gel reaction and cured at 420 °C after the spin casting on Si wafers. The refractive indices of prepared MTMS:TEOS copolymer films were measured and represented in Figure 5. When the MTMS content is increased, the refractive index of MTMS:TEOS copolymers decreases, presumably due to the fact that MTMS monomer has a methyl group bonded to a Si atom which lowers the polarity of the material. Measured refractive indices of MTMS:TEOS copolymers with 3:7, 2:9, and 1:9 molar ratio are 1.41, 1.42, and 1.45, respectively. Among the prepared MTMS:TEOS copolymers, the 1:9 copolymer was chosen for the bottom layer of broadband ARCs.

For the formation of a broadband bilayer ARC film, the MTMS: TEOS (1:9) copolymer was first spun and precured at 200 °C for 30 min before the deposition of a nanoporous organosilicate film to prevent the washout of the bottom layer during the spin casting of the top layer. After deposition and precuring of the bottom layer, an organosilicate solution containing a 40 wt % of porogens was spin-casted and cured at 420 °C for 1 h. The prepared bilayer structure was also confirmed by cross-sectional FE-SEM, as shown in Figure 6, verifying the bilayer ARC film with a nanoporous organosilicate film ($n \sim 1.23$) on top of a TEOS:MTMS (9:1) copolymer ($n \sim 1.45$). Although the nanoporous structure of the top layer is not clearly shown with the spatial resolution of FE-SEM, different textures for the top and the bottom layers are clearly visible.

The bilayer structure of the prepared broadband ARC film is tested with XRR experiments. Figure 7a shows the experimental reflectivity data with open circles and the curve fit with a solid line for the bilayer film measured in air. When we compare with the XRR data on the single porous film in Figure 3, the XRR curve for the bilayer film has an additional critical angle at $q = 0.028$, which originates from the interface between top porous and bottom dense layers, and also represents a different Kessing
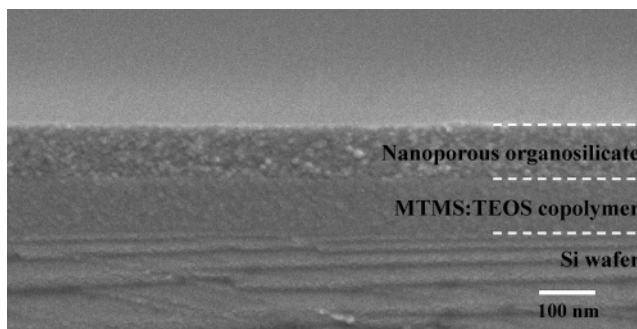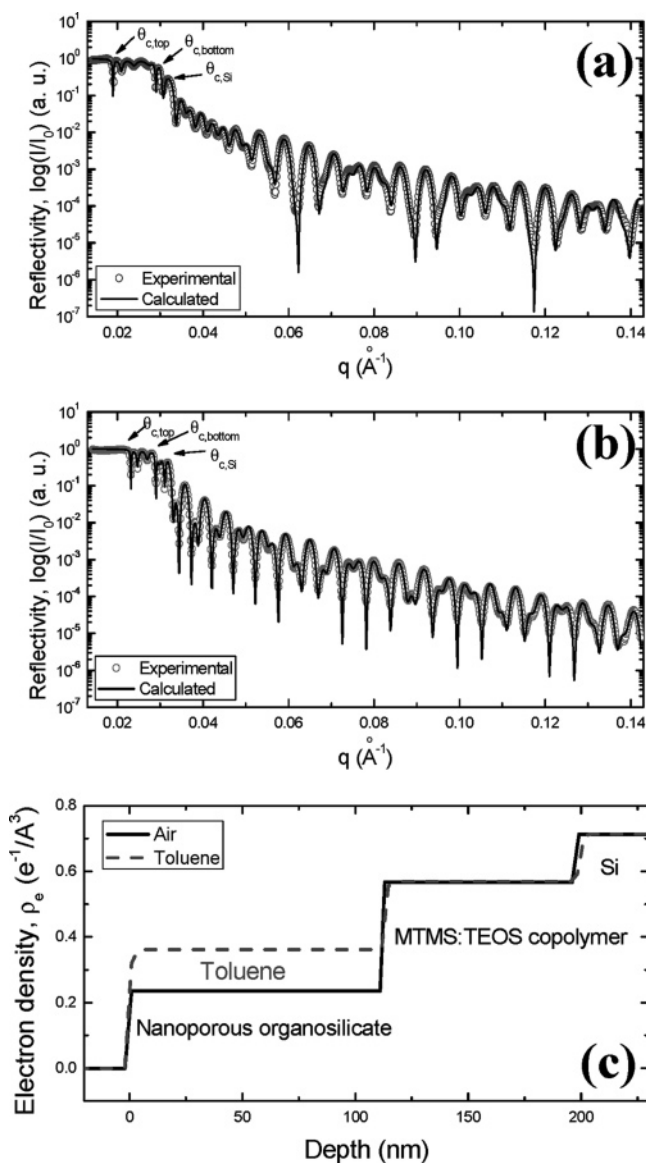

Figure 7. XRR curves for a bilayer ARC film obtained: (a) ambient conditions; (b) under saturated toluene environment. (c) Electron density profiles for the bilayer ARC measured both in air and under saturated toluene environment.

fringe pattern. The first critical angle at $q = 0.018$ is due to the nanoporous organosilicate top layer since it has the lowest average electron density. At the q region from 0.018 to 0.028, the X-ray
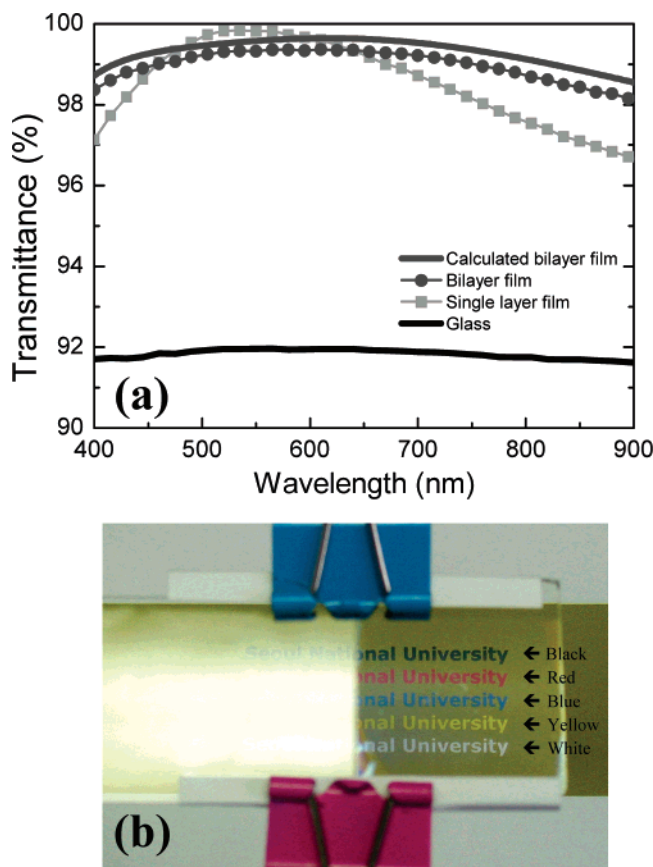
Figure 8. (a) UV−vis transmittance for the glasses coated with different types of ARCs. (b) Optical photographs of a glass without (left) and with (right) the bilayer ARC.

Table 2. Physical Properties of a Bilayer Nanoporous Film with a Nanoporous Top Layer ($n \sim 1.23$) and an Organosilicate Bottom Layer ($n \sim 1.45$) from the XRR Experiments Measured both in Air and under Saturated Toluene Environment

environment	layer	ρ_e (e^{-1}/Å^3)	density (g/cm^3)	thickness (nm)	roughness (nm)	porosity (%)
air	top	0.235	0.750	111.3	0.2	46.6
	bottom	0.568	1.811	86.0	0.3	0.4
toluene	top	0.362	1.153	113.5	0.8	
	bottom	0.569	1.814	86.0	0.8	

beam penetrates the top layer, but the X-ray beam is again reflected off the interface between the top and the bottom organosilicate layer. The fringe pattern in this region yields information on the film thickness of the top layer. The thickness for the bottom layer can be obtained by the curve fit against the complex fringe pattern above the critical angle of a silicon wafer at $q = 0.032$. Likewise, the XRR data measured after toluene sorption were also fitted. From the curve fit, electron density profiles for the bilayer film measured in air and after toluene sorption were shown in Figure 7c and the XRR curve fit results are also listed in Table 2. The major difference from the XRR data measured in air is the critical angle of the top layer since the porous top layer can only afford the sorption of toluene vapor. We also found that although we placed the bilayer film under toluene vapor over 2 h, the critical angle of the bottom layer does not vary, implying that the bottom layer is so dense that it is not swollen by the toluene sorption. Consequently, the average electron density of the bottom layer is almost intact, as shown in Figure 7c. The porosity and thickness of the top layer for the bilayer film are 46.6% and 111.3 nm, respectively, which are in good agreement with the values extracted from the single-layer
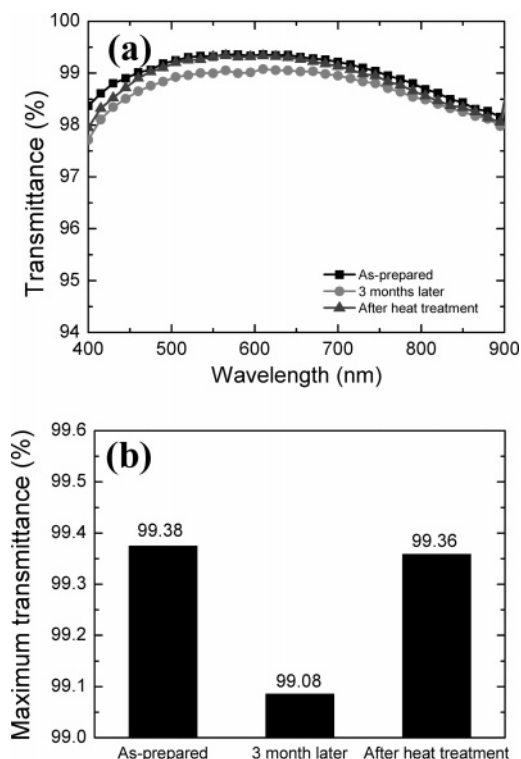

Figure 9. (a) Changes in transmittance of a glass coated with the bilayer ARC in different sample treatment conditions. (b) Change in the maximum transmittance for samples treated in different conditions.

film. The XRR experiments for the bilayer film also confirm the bilayer structure and the formation of a nanoporous top layer.

UV−vis transmittance of the glass coated with the bilayer ARC film prepared in this study was measured and compared with the case for the glass coated with the single-layer ARC film, as shown in Figure 8a. Although the bilayer ARC film shows the maximum transmittance of 99.38%, which is slightly lower than the value for the single-layer ARC film, the bilayer ARC film yields the novel broadband antireflection with 98% or higher in transmittance at wavelength ranging from 400 to 900 nm. To appreciate the effect of the broadband ARC, optical images for glasses with and without the antireflective bilayer film are shown in Figure 8b. The left hand side of a glass without ARC considerably reflects light and colored words cannot be read due to the ghost image from light. On the other hand, the ARC-coated glass shows a clear image of colored words, proving that our designed broadband AR film works well as an ARC.

Another advantage of nanoporous organosilicate ARCs is its inherent hydrophobicity and thermal stability. The hydrophilic nature of an AR film can cause water condensation in the pores of the film. The condensation of water ($n \sim 1.33$) can induce the increase in the refractive index of an ARC film and it could eventually deteriorate the AR property of the nanoporous ARC film. The hydrophobic nature of organosilicate thin films is closely linked to the durability of the AR film. To test the durability of the ARC film, we measured UV−vis transmittance after the ARC film is placed in ambient conditions for 3 months, as shown in Figure 9. The maximum transmittance decreases by 0.3% to 99.08. Although the maximum transmittance is slightly decreased, it still demonstrates a maximum transmittance over 99%, which is a signature for durable ARC films. To recover the AR property, the ARC-coated glass was subject to heat treatment at 120 °C for 10 min to remove adsorbed water. After the heat treatment, the AR property is almost recovered, showing the maximum

transmittance of 99.36%, which is almost the same value as the fresh ARC-coated glass (Figure 9).

Summary

Nanoporous organosilicate films were successfully realized by the microphase separation between an organosilicate matrix and pore-generating polymers. The refractive index of prepared nanoporous films can be adjusted and lowered down to 1.23 by incorporating the controlled amount of porogens into the matrix. Glasses coated with the nanoporous organosilicate films containing nanopores with 2−3 nm in radius show the maximum transmittance above 99.8% in the visible region. The wavelength at the maximum transmittance (λ_{max}) can be varied by different film thickness using different solution concentration. To overcome the limit in the single-layer ARC film, broadband antireflective coatings were also achieved by organosilicate bilayer films with a different combination of refractive indices and film thicknesses. ARC films based on organosilicate films show good AR durability and the reduced maximum transmittance due to the contamination with adsorbed water can be easily recovered by simple heat treatment.

LA070003Q